Materials Science Forum
ISSN: 1662-9752, Vol. 1187, pp 63-73
doi:10.4028/p-L9BoI3

Submitted: 2026-01-13
Revised: 2026-02-17
Accepted: 2026-02-19
Online: 2026-04-17

Estimation of the Lateral Gap in PECM: A Case Study on Tool Steel S390

Richard Petermann[1,a*], Gunnar Meichsner[1,b], Pascal Clauß[1,c], Steven Nickel[1,d] and Matthias Hackert-Oschätzchen[1,e]

[1]Chair of Manufacturing Technology with Focus Machining, Faculty of Mechanical Engineering,

Otto von Guericke University Magdeburg, Universitätsplatz 2, 39106 Magdeburg, Germany

[a]richard.petermann@ovgu.de, [b]gunnar.meichsner@ovgu.de, [c]pascal.clauß@ovgu.de,
[d]steven.nickel@ovgu.de, [e]matthias.hackert-oschaetzchen@ovgu.de (*corresponding author)

Keywords: PECM, Pulsed Electrochemical Machining, S390, lateral gap, working gap.

Abstract. Pulsed Electrochemical Machining (PECM) is an established process that is characterized by the machinability of metallic workpieces regardless of their mechanical properties. Applications of PECM, such as the manufacturing of punches made from hardened tool steel, often utilize the lateral working gap for the final shaping of the workpiece. A major challenge in designing an economically viable removal process is the prediction of the lateral gap for certain targeted feed rates. This case study presents a design strategy for the design of PECM applications utilizing the lateral gap. Based on a characterization of the material removal characteristics of the hardened tool steel S390, preliminary experiments were conducted to characterize the relation between the feed rate, the current density in the frontal gap as well as the voltage and the lateral gap. Further, multiple parameter sets were derived for the machining with a targeted lateral gap. The validity of these parameter sets was verified experimentally. Based on these results, a cathode for the manufacturing of a demonstration punch was designed and manufactured. These demonstration punches were machined and the resulting dimensions evaluated. Lastly, fine adjustments regarding the process parameters were applied to achieve the targeted geometric accuracy.

Introduction

Electrochemical machining (ECM) is a manufacturing process based on anodic metal dissolution. The material removal occurs contactless and regardless of the mechanical properties of the workpiece [1]. This allows the machining of thin structures and conventionally hard to machine metals such as stainless steels [2], hardened steels [3,4], titanium [5] or nickel-chromium superalloys [6].

Pulsed electrochemical machining (PECM) is an advanced variant of the general ECM process. This variant is characterized by the application of a pulsed direct current in conjunction with an oscillating cathode. A schematic of the process is displayed in Fig. 1a). The oscillation of the cathode is superimposed with the feed of the cathode. An electrolyte is flushed in the gap between the cathode (tool) and the anode (workpiece). Phase I is located around bottom dead center and characterized by the removal effective direct current pulse. Here, the workpiece material is dissolved into the electrolyte. The location and distribution of the material removal is governed by the distribution of current density. PECM increases the localization of the material removal compared to ECM, due to the reduced frontal gap as a result of the oscillation. Phase II is characterized by the widening of the gap due to the oscillation. This increase in gap aids the flushing of the electrolyte and ensures the removal of gases and removal products from the machining gap. The cycle is repeated until the desired machining depth is reached [1].

A major challenge associated with the application of PECM concerns the design of the removal device and the development of suitable process input parameters. Industrial applications are commonly designed based on personal experience. These designs are subsequently refined through empirical approaches consisting of multiple iterations of designs and process parameters. The utilization of Multiphysics simulation presents a complementary approach [8,9]. Here, the occurring physical and chemical phenomena are implemented to predict the resulting distribution of process

parameters such as the current density distribution and electrolyte flushing. The desired result is the determination of the shape of the final workpiece. Despite the obtainable insights, the accompanying cost associated with this approach limits the utilization in small and medium-sized companies.

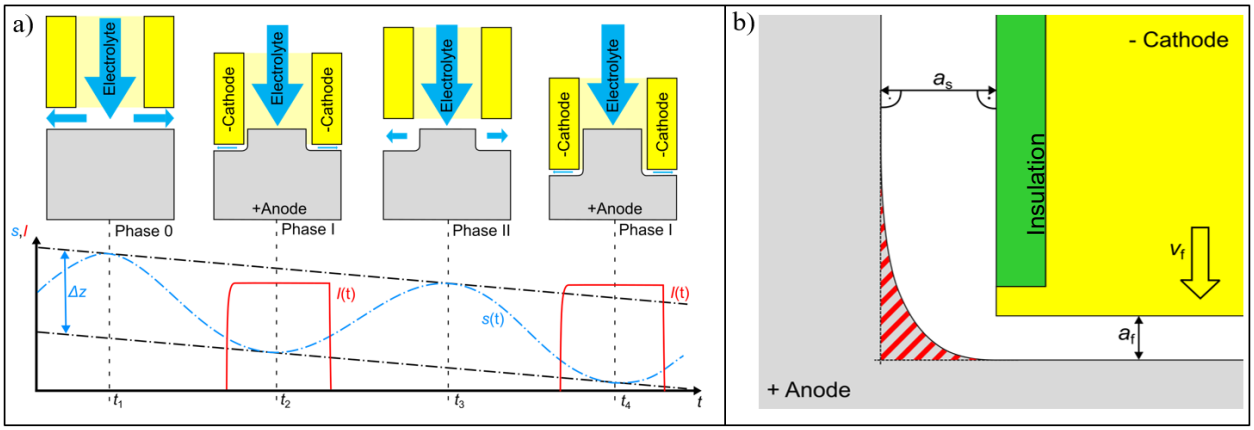

Fig. 1. a) Principle of PECM with sine oscillation and a single direct current pulse according to [3] b) Schematic of frontal gap a_f and lateral gap a_s with transition between frontal gap and lateral gap hatched with red bars according to [7]

In many applications, including the machining of punches, the final shape of the workpiece is determined by the shape of the cathode and the resulting lateral gap a_s. This lateral gap is formed when external or internal cathodes are applied. Here, the frontal gap extends around the cathode. The increased distance from the conductive surface results in a decrease in local current density and therefore in a decrease in removal rate v_a. As a result, a point of minimal material removal is reached, resulting in the creation of a surface parallel to the feed rate [1,7]. Fig. 1b) illustrates this transition between frontal gap and lateral gap and shows the frontal gap a_f and lateral gap a_s.

It is known that the resulting lateral gap is dependent on parameters such as the design of the removal device, the workpiece specific material removal characteristics, and process parameters. [1,7-10] Previous investigations showed that the relation between the resulting lateral gap a_s and the voltage U_q as well as the current density in the frontal gap J_f can be correlated with the functional relation shown by Eq. 1. [7]

$$a_s\left(J_f(v_f), U_q\right) = p_1 + p_2 \cdot J_f(v_f) + p_3 \cdot U_q + p_4 \cdot J_f(v_f) \cdot U_q \tag{1}$$

The parameters p_1 to p_4 represent coefficients, which are determined via regression based on an experimental characterization of the lateral gap. These parameters are specific to the cathode, the workpiece material and selected process input parameters. The current density in the frontal gap J_f is derived based on the feed rate v_f of the cathode. The functional relation is derived during experimental material removal characterizations. The relation is commonly described by linear functions in the format presented in Eq. 2 [2,4,11]. The parameters $V_{f,m}$ and $v_{f,0}$ are the determined regression coefficients.

$$v_f(J_f) = V_{f,m} \cdot J_f + v_{f,0} \tag{2}$$

A previous study [4] investigated the removal characteristics of the hardened powder metallurgical tool steel S390. This case study applies the presented findings and derives input parameters for the characterization of the lateral gap based on these previous findings. Fig 2 displays the obtained relation between the feed rate v_f and the current density J. Three distinct areas are seen, which were correlated with linear functions in the format of Eq. 2. The parameters of these functions are summarized in Table 1. [4]

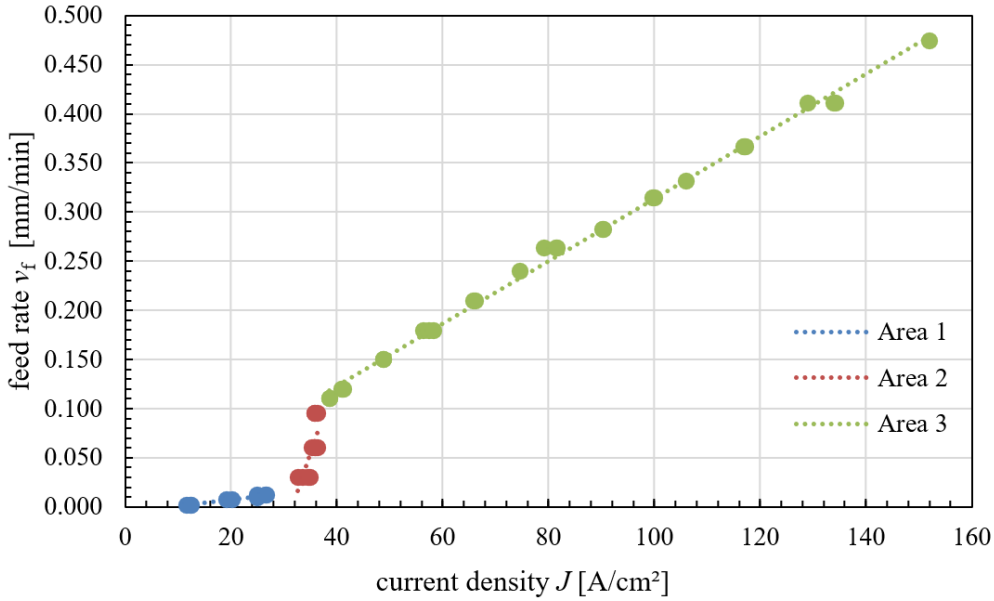

Fig. 2. Feed rate v_f as a function of the current density J for PECM of S390 with a frequency of 50 Hz and a pulse width of 4 ms according to [4]

Table 1. Parameters of the correlation functions v_f (J) for the material removal of S390 with a frequency of 50 Hz and a pulse width of 4 ms according to [4]

Area	J [A/cm²]	$V_{f,m}$ [mm/min / A/cm²]	$v_{f,0}$ [mm/min]
1	12 – 30	0.0007	-0.0066
2	33 – 36	0.0162	-0.5116
3	38 – 117	0.0033	-0.0093

The hardened tool steel S390 was investigated as it represents the class of powder metallurgical steels. The samples were hardened to a hardness of 890 ± HV_{30} [4]. Major alloying components are tungsten (10.4 %), cobalt (8.0 %), vanadium (4.8 %) and carbon (1.64 %) [4]. It is to note that around 10 % of the material consists of Fe_3W_3C and VC carbides [12]. Common applications of S390 are cutting tools such as skiving wheels as well as punches [4].

This study showcases a systematic approach for the design of removal devices. In contrast to the common empirical approach, a characterization of the lateral gap was initially performed. Based on this characterization, a removal device was designed. The device is then applied and the parameters were adjusted, utilizing the insights obtained from the lateral gap characterization.

Methodology

This case study presents a novel approach for the development of removal devices for PECM. For this purpose, a device for the manufacturing of punching dies consisting of S390 was designed and trialed. In order to design the final dimensions of the cathode, an initial characterization of the lateral gap was conducted. Based on a general characterization of the material removal (see [4]), experiments were designed and conducted in order to derive an analytical model of the lateral gap (see Eq. 1) [7]. Based on this analytical model, several combinations of feed rate v_f and voltage U_q were derived to achieve a targeted lateral gap. The results were then applied to machine a cloverleaf geometry with a targeted lateral gap. Lastly fine adjustments to the parameter set were performed to achieve the desired geometric accuracy. The individual steps are summarized by Table 2.

Table 2. Summary of the conducted steps

Step	Description	Results
1	Material removal characterization (see [4])	• Correlation v_f (J_f) • Parameter combinations of v_f and U_q which result in frontal gaps in the range from 10 µm to 100 µm.
2	Characterization of the lateral gap	
2.1	Initial Experiments (series 1) →experiments applying known parameter combinations from step 1	• General overview regarding the resulting lateral gap and frontal gap
2.2	Additional experiments (series 2) → Investigation of additional supporting points (v_f, U_q)	• Sufficient experimental data set consisting of input parameters (v_f, $J_f(v_f)$, U_q) and the resulting lateral gaps a_s.
2.3	Derivation of the mathematical model → Correlation of the parameters p_1 to p_4 to the experimental data	• Analytical description of the lateral gap (see Eq. 1)
2.4	Investigation of parameter combinations resulting in a constant lateral gap (series 3)	• Experimentally validated parameter sets for a nearly constant lateral gap
3	Design of the removal device → Assumption of a constant lateral gap based on the results of 2.4	• Designed and manufactured removal device
4	Commissioning of the removal device	
4.1	Initial experiments → Experiments applying the removal device of 3 with previous parameter sets from 2.4	• Resulting geometric accuracy
4.2	Fine adjustment → Adjustment of the voltage based on a targeted change in lateral gap	• Final parameter set • Validated reproducibility

Experimental Setup. All experiments were conducted applying a commercial machine tool PEM 800 S by PEMTec. Fig. 3 presents the applied removal device. The characterization of the lateral gap was conducted by applying a cylindrical cathode made from stainless steel AISI 304. A cylindrical sample geometry with a diameter of 12 mm was chosen for the anode material. The lateral gap was derived based on the diameter of the cathode and the resulting diameter of the anode, as shown by Eq. 3 [7].

$$a_s = \frac{D_{cathode} - D_{anode}}{2} \tag{3}$$

The dimensions of the cylindrical cathode are summarized in Table 3 The upper surfaces of the cathode are insulated. The electrolyte is flushed from top to bottom as indicated in Fig. 3. A flushing chamber is incorporated, allowing the outlet of the electrolyte to be pressurized. The pressure at the outlet p_{out} was created by applying a valve with an opening of 4 %. The dimensions of the cathode were measured applying a coordinate measuring machine (CMM) PMM 886 by Leitz. The samples were measured applying a micrometer IP65-0-25 by Mitutoyo. An underestimation of the lateral gap by an average of 1.4 µm compared to the values obtained applying a CMM is expected based on results discussed by a previous investigation [10]. The error is deemed acceptable when weighed against the associated reductions in cost and processing time, particularly in view of the method's industrial applicability.

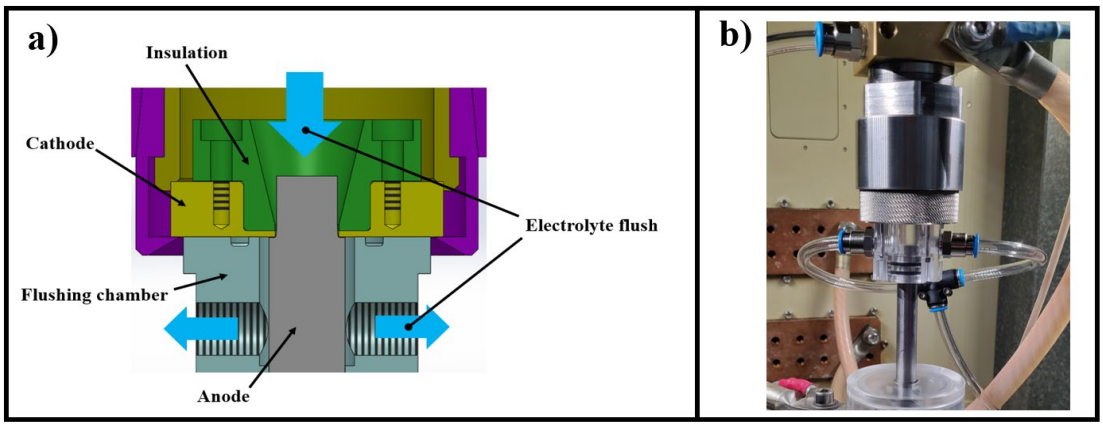

Fig. 3.a) Sectional representation of the removal device with illustration of the flushing direction [7] b) Removal device in the machine tool

Table 3. Characteristic parameters of the cylindrical cathode [7]

Parameter	Symbol	Value
Material		AISI 304 (X5CrNi18-10 or 1.4301)
Diameter	$D_{cathode}$	10.0090 [mm]
Roundness	$R_{cathode}$	0.0086 [mm]
Height	$h_{cathode}$	0.923 [mm]

Design of Experiments. Several parameters were kept constant throughout all experiments. The frequency f_{osc} of 50 Hz and the pulse width t_p of 4 ms were selected based on the previous material removal characterization [4]. An anode diameter of 12 mm was selected. The electrolyte was flushed from the lateral gap (top) into the frontal gap (bottom), as visualized by Fig. 3. An electrolyte inlet pressure p_{in} of 600 kPa was selected. A constant valve opening of 4 % was applied at the outlet, resulting in a pressure at the outlet p_{out} in the range between 190 kPa and 400 kPa depending on the resulting gap. A machining depth s of 6 mm was selected. This presents a reduction of 2 mm compared to previous investigations [7,10] in order to reduce the machining time. A $NaNO_3$ electrolyte with around 8 % mass fraction was applied. The constant parameters are summarized in Table 4.

The objective of this case study is the design of a removal device and process parameter set for the manufacturing of punches. Analyzing the removal characteristics of the S390 (see Fig. 2), it is decided to investigate current densities in the frontal gap above 40 A/cm^2. This removal area is characterized by feed rates above 0.100 mm/min, making this area economically viable. Based on previous investigations [7,10], it is assumed that the lateral gap can be described by a singular parameter set p_1 to p_4 (see Eq. 1) for current densities above 40 A/cm^2, as this area is characterized by a current efficiency above 80 % (see [4]). Further, the formation of an area of minimal lateral gap is expected in the range between 30 A/cm^2 and 40 A/cm^2, due to the characteristic change in current efficiency.

Table 4. Constant machining parameters

Parameter	Symbol	Value
Electrolyte $NaNO_3$ (aq)		8 [% mass fraction]
Electric conductivity	σ	67 [mS/cm]
Electrolyte temperature	T_{el}	20 [°C]
Machining depth	s	6 [mm]
Electrolyte inlet pressure	p_{in}	600 [kPa]
Outlet valve opening		4 [%]
Oscillation frequency	f_{osc}	50 [Hz]
Oscillation amplitude	h_{osc}	200 [µm]
Pulse width	t_p	4 [ms]

The initial 7 experiments were designed with current densities in the range between 40 A/cm^2 and 150 A/cm^2. The voltages were selected based on prior experiments (see [4]). Additional 3 experiments with current densities between 25 A/cm^2 and 35 A/cm^2 were conducted, to verify the existence of a minimal lateral gap.

The second series of experiments was comprised of 8 additional experiments with 50 A/cm^2, 100 A/cm^2 and 150 A/cm^2 applying a wider range of voltage. The ranges of the variable parameters are summarized in Table 5.

Table 5. Variable parameters of the first and second experimental series

Series	Parameter	Symbol	Range
1	Voltage	U_q	5.6 [V] – 18.2 [V]
	Feed rate	v_f	0.011 [mm/min] – 0.486 [mm/min]
	Current density in the frontal gap	J_f	25 [A/mm^2] – 150 [A/mm^2]
2	Voltage	U_q	7.7 [V] – 21.0 [V]
	Feed rate	v_f	0.156 [mm/min], 0.222 [mm/min], 0.486 [mm/min]
	Current density in the frontal gap	J_f	50 [A/mm^2], 100 [A/cm^2], 150 [A/mm^2]

Lateral Gap Characterization

The resulting lateral gaps of the initial series of experiments are presented in Fig. 4 (left) as a function of the voltage. The graph is divided by applying a current density threshold of $J_f = 40$ A/cm^2. This threshold coincides with the change in the removal characteristics as previously discussed.

A nearly linear increase of the lateral gap with increasing voltage is seen for current densities above 40 A/cm^2. The gap increases from around 105 µm at 7.7 V to around 260 µm at 18.2 V. Three experiments were conducted with current densities below 40 A/cm^2. The resulting lateral gap ranges from around 140 µm at 5.6 V to 95 µm at around 6.3 V clearly breaking with the trend seen above 40 A/cm^2. An area of minimal lateral gap seems to form around current densities of 40 A/cm^2. This observation is consistent with [7], where an area of minimal lateral gap was found in the area of the characteristic change in current efficiency in the frontal gap.

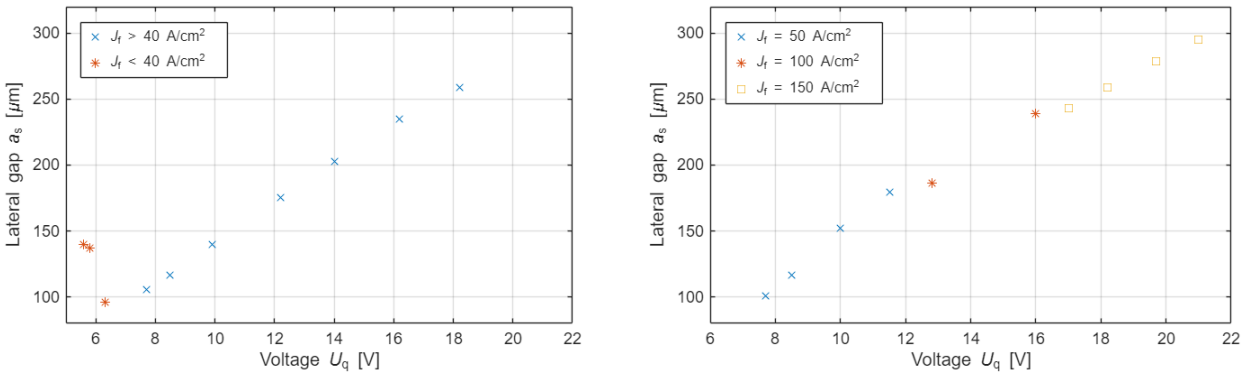

Fig. 4. Resulting lateral gap a_s as a function of the voltage U_q for varying current densities J_f (left) and resulting lateral gap a_s as a function of the voltage U_q for selected current densities J_f (right)

The diagram on the right side of Fig. 4 displays the lateral gap of the second experimental series as a function of the voltage. A linear increase of the lateral gap with increasing voltage is seen for all current densities. The resulting lateral gaps for current densities above 40 A/cm^2 are correlated with a function in the format of Eq. 1. The resulting parameters are summarized in Table 6. A degree of determination R^2 of 99.8 % was reached. Additionally, the root mean squared deviation (RMSE) was

evaluated. The RMSE describes quadratic mean deviation of the correlation function $a_s(J_f, U_q)$ from the experimental results. A RMSE of 3.4 µm was derived.

Table 6. Parameters of the correlation function (1) $a_s(J_f,U_q)$ for $J_f > 40$ A/cm^2

p_1 [µm]	$p_2 \left[\frac{\mu m}{\frac{A}{cm^2}}\right]$	$p_3 \left[\frac{\mu m}{V}\right]$	$p_4 \left[\frac{\mu m}{\frac{A}{cm^2} \cdot V}\right]$
-51.4410	0.1954	20.6655	-0.0358

Considering the observed lateral gaps, a target lateral gap of 220 µm was chosen for the design of a removal device to explore a broad range of parameter combinations. The process input parameter combinations of feed rate v_f and voltage U_q were derived based on a selected range of current densities. For the purposes of this investigation, current densities between 70 A/cm^2 and 150 A/cm^2 were investigated in intervals of 10 A/cm^2. The resulting feed rates of the subsequent experiments were calculated applying Eq. 2 in conjunction with the parameters presented in Table 1. Eq. 4 presents Eq. 1 solved for the voltage, allowing the derivation of voltages for the subsequent experiments based on the selected current densities J_f and targeted lateral gap a_s.

$$U_q(a_s, J_f) = \frac{a_s - p_2 \cdot J_f - p_1}{p_4 \cdot J_f + p_3} \tag{4}$$

The resulting parameter ranges of the third experimental series are summarized in Table 7.

Table 7. Parameter ranges of the third experimental series

Series	Parameter	Symbol	Range
3	Targeted lateral gap	$a_{s\text{-target}}$	220 µm
	Voltage	U_q	14.2 [V] – 15.8 [V]
	Feed rate	v_f	0.222 [mm/min] – 0.486 [mm/min]
	Current density in the frontal gap	J_f	70 [A/cm^2] – 150 [A/cm^2]

Fig. 5 displays the resulting lateral gaps of the third experimental series as a function of the voltage. The targeted lateral gap of 220 µm is indicated by a dotted line. Lateral gaps in the range from 217 µm to 227 µm are observed. Further, the experiments in the range from 14.2 V to 15.4 V result in deviations of +/- 3 µm from the targeted lateral gap.

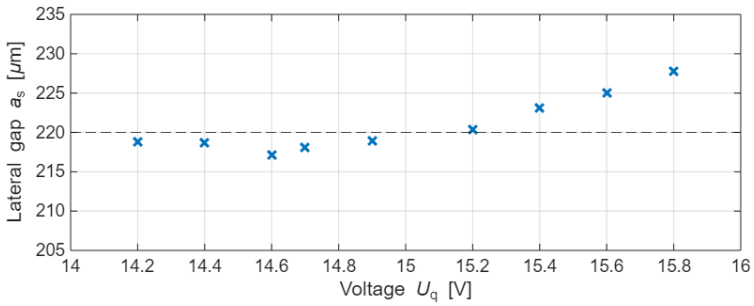

Fig. 5. Resulting lateral gaps a_s of the third experimental series as function of the voltage U_q with indication of the targeted lateral gap of 220 µm

Design of the Removal Device and Application

Building upon the process input parameters and targeted lateral gap determined in the preceding section, this chapter presents the design of a removal device. The removal device is tailored for the

machining of punches with a cloverleaf-shaped contour. The general concept of the removal device is based on the previous setup (see Fig. 3).

Fig. 6a) displays the dimensions of the punch (anode). Additionally, the corresponding shape of the cathode is visualized around the contour of the punch. The characteristic radius of the cloverleaf is designed to 1.800 mm ± 0.005 mm. Based on the targeted lateral gap of 220 µm or 0.220 mm the corresponding radius of the cathode is planned as 2.020 mm.

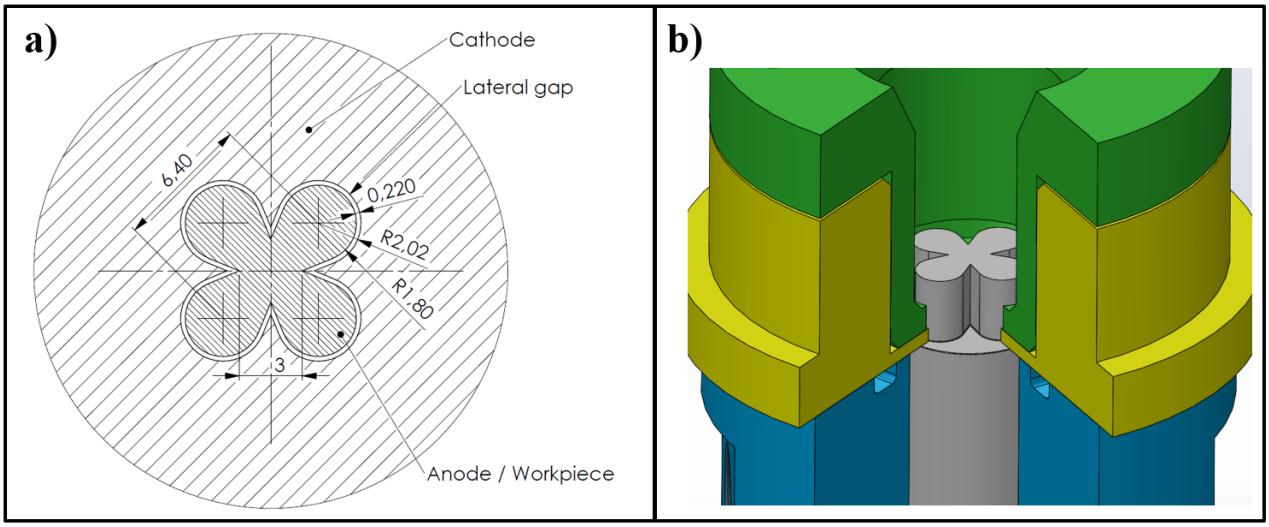

Fig. 6. a) Geometry of the punch and corresponding cathode and b) sectional representation of the designed removal device

Fig. 6b) shows a sectional representation of the designed removal device. The resulting punch is additionally displayed. The cathode (yellow) is machined to a height of 0.981 mm. Similar to the removal device applied for the initial experiment, the upper surface of the cathode is insulated (displayed green). The shape of both the cathode and the machined samples was measured by applying an optical coordinate measuring machine Bruker Alicona µCMM. An average radius of 2.018 mm was measured. Fig. 7a) displays the machined cathode.

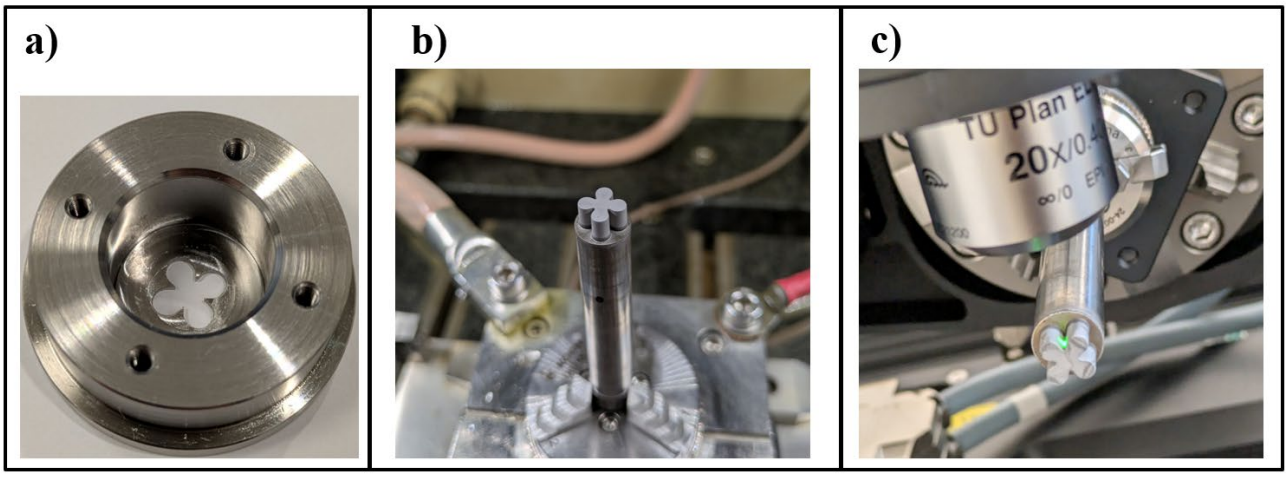

Fig. 7. a) Applied cathode with cloverleaf structure, b) Machined punch c) Optical measurement of a machined punch

Initial Experiments. Based on the previous characterization of the lateral gap, 3 sets of parameters were derived and applied for the machining of the demonstration punches. In total, 6 punches (2 experiments per parameter set) were machined. An image of a machined punch is displayed in Fig. 7b).

The applied parameters are summarized in Table 8. The resulting average radius of the leaves as well as the resulting frontal gap of the experiments are additionally displayed. The resulting

geometries were evaluated by investigating the achieved radii of the “leaves”. The measurements revealed radii in the range of 1.74 mm to 1.75 mm, compared to the specified radius of 1.800 mm.

Table 8. Parameter sets for the manufacturing of the punches

Parameter set	1	2	3
Feed rate [mm/min]	0.222	0.321	0.420
Voltage [V]	14.2	14.7	15.4
Frequency [Hz]	50	50	50
Pulse width [ms]	4	4	4
Machining depth [mm]	6	6	6
Average Radius of the leaves [mm]	1.751	1.749	1.741
Resulting frontal gap [µm]	44	30	27

Fine adjustment. The radii of the initial experiments are deviating by around - 0.05 mm from the specified radius. In order to increase the radii to 1.8 mm ± 0.005 mm, a reduction in lateral gap of - 0.05 mm is needed. As described by [7], a reduction in lateral gap can be achieved by a) an increase in feed rate/current density in the frontal gap or b) a decrease in voltage. These adjustments both are commonly accompanied by a reduction in frontal gap [1,11]. Therefore, parameter set 1 was selected for further investigation, as the previous experiments resulted in the largest frontal gaps with 44 µm compared to set 2 with 30 µm and set 3 with 27 µm, respectively.

The effect of a change in voltage on the lateral gap for a certain current density in the frontal gap can be approximated by the factor $p_U(J_f)$ (see Eq. 5). The relation is derived from Eq. 1 as demonstrated by [7].

$$p_U(J_f) = p_3 + p_4 \cdot J_f \tag{5}$$

Applying a current density J_f of 70 A/cm^2 results in a factor p_U of 18.16 µm/V. The estimated change in voltage ΔU_q needed for a change in lateral gap Δa_s is derived by applying Eq. 6.

$$\Delta U_q = \frac{\Delta a_s}{p_U} \tag{6}$$

The initial adjustment is planned based on a targeted decrease of lateral gap of Δa_s = -50 µm. An initial adjustment of ΔU_q = - 2.7 V was derived by applying Eq. 6. As a result, parameter set 1.1 was defined based on parameter set 1, applying a voltage U_q = 11.5 V. An average radius of 1.808 mm was obtained.

A second adjustment of ΔU_q = + 0.5 V was applied in order to slightly decrease the radius of the cloverleaves. Parameter set 1.2 is defined by applying a voltage of U_q = 12.0 V resulting in a measured average radius of 1.802 mm. The specified range of 1.800 mm± 0.005 mm was therefore reached. Four additional experiments were conducted applying parameter set 1.2. The measurements of all 5 samples revealed average radii in the range between 1.800 mm and 1.804 mm satisfying the specified tolerance of 1.800 mm ± 0.005 mm. The adjustments and resulting radii are displayed in Fig. 8. The error bars indicate the minimal and maximal radius of each sample.

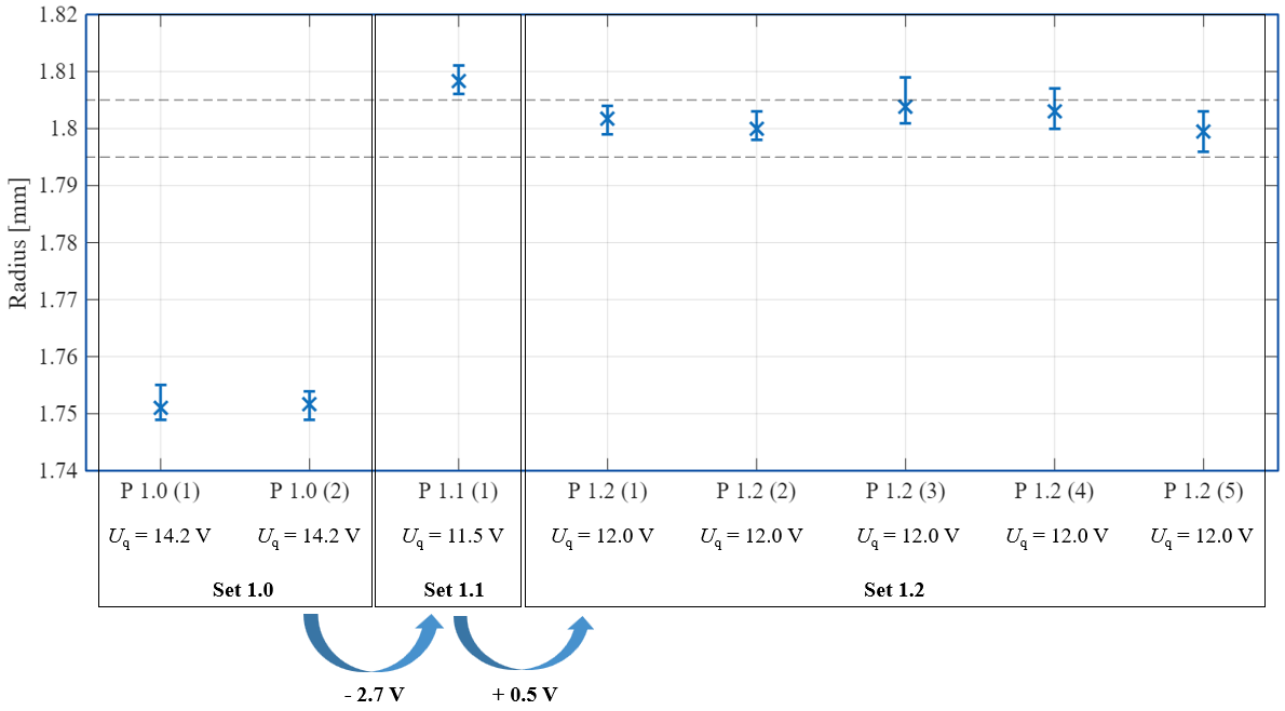

Fig. 8. Visualization of the resulting radii of the cloverleaves as a result of the fine adjustment of the voltage with indication of the average, minimal, and maximal obtained radius of each sample

Discussion and Outlook

The initial characterization of the lateral gap validated the applicability of the previously developed model of the lateral gap a_s (J_f, U_q). Here the area of current efficiency above 80 % correlated with an achieved RMSE of 3.4 µm. The model was then applied to derive multiple parameter sets targeting a certain, fixed lateral gap. A number of input parameter combinations (feed rate and voltage) were experimentally investigated, resulting in deviations between – 3 µm and + 7 µm from the targeted lateral gap.

A cathode for the machining of punches with a cloverleaf shape was designed and manufactured. The transfer of parameter sets for the initial experiments to the new cathode resulted in measurable deviations in the radii of the leaves. The radii were around -0.05 mm to – 0.06 mm smaller than specified, indicating an increased material removal and lateral gap compared to the estimation.

An initial adjustment of the voltage resulted in a significant reduction in the observed deviations. The estimation of the needed adjustment showed a promising approach for the fine tuning of process parameters for industrial applications. Following a second adjustment, the target radius was successfully achieved, satisfying the specified tolerance of ± 0.005 mm.

The deviations between the initial characterization of the lateral gap and the machining of the punches indicate that the shape of the cathode has a major influence on the forming gap and therefore on the resulting geometry of the workpiece. The effect of the shape of the cathode, especially the shape of the inner conductive surface, is currently not yet sufficiently investigated. As previously stated, the applied model for the characterization of the lateral gap is specific to the applied cathode.

The existence of multiple process input parameter combinations resulting in a constant lateral gap presents an important result for the design of PECM applications. This should theoretically enable a fine tuning of removal processes targeting aspects such as the productivity (via the feed rate) or process stability (focusing on the frontal gap and the flushing of the gap) while maintaining a fixed lateral gap. The existence of a minimal lateral gap further validates the observations made by [7].

Acknowledgements

The machine tool PEM 800 S is funded by the German Research Foundation (DFG) with project number 467011871.

References

[1] F. Klocke, W. Koenig, Fertigungsverfahren Band 3. Springer Verlag, 2007. https://doi.org/10.1007/978-3-540-48954-2

[2] G. Meichsner, M. Hackert-Oschätzchen, M. Krönert, J. Edelmann, A. Schubert, M. Putz, Fast Determination of the Material Removal Characteristics in Pulsed Electrochemical Machining, Procedia CIRP 46 (2016) 123-126. https://doi.org/10.1016/j.procir.2016.03.175

[3] A. Schubert, G. Meichsner, M. Hackert-Oschätzchen, M. Zinecker, J. Edelmann, Pulsed electrochemical machining of powder metallurgy steels, 7th International Symposium on Electrochemical Machining Technology (2011), pp. 68–75. https://doi.org/10.24406/publica-fhg-372620

[4] R. Petermann, P. Clauß, P. Damm, G. Meichsner, M. Hackert-Oschätzchen, Experimental Derivation of Process Input Parameters for Electrochemical Precision Machining of a Power Metallurgical Tool Steel, Materials Research Proceedings 41 (2024), https://doi.org/10.21741/9781644903131-260

[5] F. Klocke, T. Herrig, M. Zeis, A. Klink, Experimental Research on the Electrochemical Machinability of selected γ-TiAl alloys for the manufacture of future Aero Engine Components, Procedia CIRP 35 (2015) 50-54. https://doi.org/10.1016/j.procir.2015.08.050

[6] A. Frank, T. Hall, M. Zeiner, D. Bähre, Study of Pulse Electrochemical Machining on Conventionally and Additively Manufactured Inconel 718 Workpieces, 20th International Symposium on Electrochemical Machining Technology (2024) 11-19. https://doi.org/10.18154/RWTH-2024-10230

[7] R. Petermann, P. Clauß, G. Meichsner, F. Meyer, M. Hackert-Oschätzchen, Experimental characterisation of lateral machining gap during Pulsed Electrochemical Machining for corrosion resistant tool steel, Procedia CIRP 137 (2025) 306-311, https://doi.org/10.1016/j.procir.2025.06.009

[8] F. Böttcher, I. Schaarschmidt, J. Edelmann, A. Schubert, Simulation-Assisted Tool Design for Pulsed Electrochemical Machining of Magnetic Shape-Memory Alloys, J. of Manufacturing and Materials Processing 8 (2024). https://doi.org/10.3390/jmmp8020046

[9] I. Schaarschmidt, M. Hackert-Oschätzchen, G. Meichsner, P. Steinert, M. Zinecker, A. Schubert, Working Gap Analysis in Electrochemical Precision Machining of External Geometries with Ring Cathodes, Procedia CIRP 95 (2020) 662-667, https://doi.org/10.1016/j.procir.2020.02.279

[10] R. Petermann, P. Clauß, G. Meichsner, F. Meyer, S. Nickel, M. Hackert-Oschätzchen, Analysis of repeatability for experimental characterization of lateral gap during Pulsed Electrochemical Machining, 21th International Symposium on Electrochemical Machining Technology (2025) 57-64, https://doi.org/10.51382/978-3-96100-259-7-07

[11] G. Meichsner, A. Schubert, Entwicklung und Realisierung einer Methode zur Bestimmung von Prozesseingangsgrößen für das elektrochemische Präzisionsabtragen, PhD Thesis, Scripts Precision and Microproduction Engineering 12 (2018), ISBN 9783957350879

[12] H. Peng, L. Hu, L. Li, L. Zhang, X. Zhang, Evolution of the microstructure and mechanical properties of powder metallurgical high-speed steel S390 after heat treatment, Journal of Alloys and Compounds 740 (2018) 766-773. https://doi.org/10.1016/j.jallcom.2017.12.264